CD133 expression in osteosarcoma and derivation of CD133+ cells

JI LI[1*], XIAO-YAN ZHONG[2*], ZONG-YU LI[3], JIN-FANG CAI[3], LIN ZOU[3], JIAN-MIN LI[4], TAO YANG[5] and WEI LIU[6]

[1]Department of Orthopedics, The Fourth People's Hospital of Jinan/The Jinan Military General Hospital, Jinan 250031; [2]Clinical Laboratory, The Eighth People's Hospital of Jinan, Jinan 250014; [3]Department of Orthopedics, The Jinan Military General Hospital, Jinan 250031; [4]Department of Orthopedics, Qilu Hospital Shandong University, Shandong 250012; [5]Shandong Medical Association, Shandong 250014; [6]Affiliated Hospital of Shandong Traditional Chinese Medicine University, Shandong 250012, P.R. China

Received August 19, 2012; Accepted November 30, 2012

DOI: 10.3892/mmr.2012.1231

Abstract. Cluster of differentiation 133 (CD133) is recognized as a stem cell marker for normal and cancerous tissues. Using cell culture and real-time fluorescent polymerase chain reaction, CD133 expression was analyzed in osteosarcoma tissue and Saos-2 cell lines. In addition, cancer stem cell-related gene expression in the Saos-2 cell line was determined to explore the mechanisms underlying tumorigenesis and high drug resistance in osteosarcoma. $CD133^+$ cells were found to be widely distributed in various types of osteosarcoma tissue. Following cell culture, cells entered the G_2/M and S cell cycle stages from G_0/G_1. Levels of $CD133^+$ cells decreased to normal levels rapidly over the course of cell culture. Colony forming efficiency was higher in the $CD133^+$ compared with the $CD133^-$ subpopulation of Saos-2 cells. Expression levels of stem cell-related genes, including multidrug resistance protein 1 (MDR1) and sex determining region Y-box 2 (Sox2) in the $CD133^+$ subpopulation of cells were found to be significantly higher compared with the $CD133^-$ subpopulation. These observations indicate that $CD133^+$ Saos-2 cells exhibit stem cell characteristics, including low abundance, quiescence and a high potential to undergo differentiation, as well as expression of key stem cell regulatory and drug resistance genes, which may cause osteosarcoma and high drug resistance.

Correspondence to: Dr Jian-Min Li, Department of Orthopedics, Qilu Hospital, Shandong University, 107 Wenhuaxi Road, Jinan, Shandong 250031, P.R. China
E-mail: gklijianmin@yahoo.com.cn

Dr Jin-Fang Cai, Department of Orthopedics, The Jinan Military General Hospital, 50 Shifan Road, Jinan, Shandong 250031, P.R. China
E-mail: Drcaijf@163.com

*Contributed equally

Key words: osteosarcoma, cancer stem cell, multidrug resistance

Introduction

An increasing number of studies are reporting that tumors often originate from the transformation of normal stem cells. It has been hypothesized that similar signaling pathways regulate self-renewal in stem and cancer cells and cancer cell populations may themselves include cancer stem cells, rare cells with indefinite potential for self-renewal that drive tumorigenesis (1-5). Goodell *et al* (6) identified a group of Hoechst 33342-stained bone marrow cells exhibiting cancer stem cell characteristics, these cells were termed side population (SP) cells. Despite the development of surgical and chemical therapies for the treatment of osteosarcoma, the long-term survival rate associated with this disease remains at 65% (7). Multidrug resistance is a major determinant of clinical outcome in osteosarcoma (8-12). Gibbs *et al* (13) isolated osteosarcoma stem cells from an osteosarcoma cell population and found that these stem cells overexpressed key regulatory genes present in embryonic stem cells, including octamer-binding transcription factor 4 (Oct4), sex determining region Y-box 2 (Sox2) and Nanog. The authors hypothesized that expression of these genes may be a main feature of cancer stem cells. Cluster of differentiation 133 (CD133) is recognized as a stem cell marker for normal and cancerous tissues. At present, CD133 alone or in a combination with additional markers is used for the isolation of stem cells from numerous tissues, including bone marrow (14), brain (15), kidney (16), prostate (17), liver (18), pancreas (19) and skin (20). Furthermore, in a number of previous studies, monoclonal antibodies against CD133 have been used for the identification and isolation of putative cancer stem cell populations from malignant tumors of the brain, prostate (21), liver (22), pancreas (23) and lung (24). Currently, surface markers on cancer stem cells of osteosarcoma have yet to be defined. The present study investigated CD133 expression in osteosarcoma and Saos-2 cell lines to explore the underlying mechanisms of tumorigenesis and drug resistance in osteosarcoma.

Materials and methods

Immunohistochemistry and cell count analysis in osteosarcoma. All procedures were performed in accordance with

institutional guidelines from the Fourth People's Hospital of Jinan (Shandong, China) and the Department of Pathology in Qilu Hospital (Shandong, China). A total of 55 patients diagnosed with osteosarcoma, including 4, 13, 12 and 26 cases of parosteal, fibroblastic, chondroblastic and osteoblastic osteosarcomas, respectively, from the Department of Pathology (Qilu Hospital) were selected for the study. Osteosarcoma types were termed groups 1-4, respectively. Tumor tissues were removed and sent for paraffin embedding. Informed consent was obtained from all patients.

Paraffin-embedded tissue samples were routinely prepared, producing 3-μm tissue sections mounted on slides. Sections were fixed with paraformaldehyde, slides were washed 3 times for 3 min in PBS and then endogenous peroxidase activity was blocked using 1% H_2O_2. Citrate Antigen Retrieval Buffer (Beijing Zhongshan Goldenbridge Biotechnology, Beijing, China) was used to retrieve antigens and then CD133 mouse anti-human antibody (Beijing Biosynthesis Biotechnology, China) was added to sections and incubated at 37˚C for 60 and 15 min, respectively, according to the manufacturer's instructions for the SP9000 immunohistochemical kit (Beijing Zhongshan Goldenbridge Biotechnology). DAB (Fuzhou Maixin Biotechnology Development Co., Ltd., Fuzhou, China) was added to develop staining and slides were observed under a microscope. Hematoxylin staining (Beijing Zhongshan Goldenbridge Biotechnology) was performed and slides were observed under a light microscope.

Positive cell count analysis. Each section was analyzed by two observers and judged by a double-blind method. Twelve high-power fields were randomly selected under microscope for immunohistochemical staining. Sections were scored according to the following criteria: i) no color in cytoplasm, 0; ii) cytoplasm presented light yellow cloudiness, (+); iii) cytoplasm presented yellow granular state, (++); iv) cytoplasm presented uniform deep yellow, (+++). (++) and (+++) were considered positive cells and the percentage of positive cells in each section was calculated.

Saos-2 cell culture and immunohistochemitry. The Saos-2 osteosarcoma cell line was purchased from the American Type Culture Collection (Manassas, VA, USA). Cells were cultured in low-glucose DMEM (Hyclone, Logan, UT, USA) containing 10% fetal bovine serum (FBS; Hangzhou Sijiqing Biological Engineering Materials Co., Ltd., Hangzhou, China) and incubated in a 37˚C, 5% CO_2 incubator. Cells were digested with trypsin and passaged every 3 days.

Saos-2 cells in logarithmic growth phase were inoculated to prepare cell-attached coverslips and slides were prepared as described for osteosarcoma tissue samples.

CD133 flow cytometry and isolation. Saos-2 cells in logarithmic growth phase were digested with trypsin (Sino-American Biotechnology, Guangzhou, China), centrifuged, collected and washed twice with PBS. Samples were then centrifuged and the supernatant was removed. Pellets were resuspended in 5 ml PBE buffer from a magnetic bead kit (Miltenyi Biotec Ltd., Surrey, UK), filtered using a 100 mesh screen to obtain a single cell suspension and then centrifuged at 1,000 rpm for 5 min. The supernatant was removed and 100 μl antibody-coated magnetic beads/1x10^7 cells was added and incubated for 15 min at room temperature under dark conditions, followed by 2 washes in combining buffer. Cells were resuspended in 500 μl combining buffer and separated on a magnetic separation column (Miltenyi Biotec Ltd.). Fractions were collected from the column and dead cells in the original cell suspension were filtered by the column and removed.

Cells were collected, washed twice with PBS at 4˚C and the cell concentration was adjusted to 1x10^6/ml. Cell suspension (100 μl) was put into 5 ml flow tubes and then 20 μl CD133-PE monoclonal fluorescent antibody was added and incubated for 30 min at 4˚C under dark conditions. Tubes were washed twice with 5 ml PBS, centrifuged, the supernatant was removed and the precipitate was resuspended in 0.5 ml PBS. Samples were analyzed using a FACSCalibur flow cytometer (BD Biosciences, San Jose, CA, USA). CD133-PE flow fluorescence detection antibody was purchased from Miltenyi Biotec Ltd.

Population magnetic bead separation of the Saos-2 cell line. Cell suspension was collected as described and centrifuged for 5 min at 1,000 rpm. The supernatant was removed, 100 μl CD133 monoclonal antibody was added to directly label the magnetic beads and 400 μl PBE was added, mixed and incubated for 30 min at 4˚C under dark conditions. Uncombined magnetic beads were removed by two PBS washes and the pellet was resuspended in 500 μl PBE and separated on a magnetic separation column (Miltenyi Biotec Ltd.). Column flow-through contained CD133 cells. Cells retained by the column were washed with PBE and collected, these cells were $CD133^+$ cells. $CD133^+$ subpopulation cells were labeled using CD133-PE fluorescent antibody and purity was determined by flow cytometry.

$CD133^{+/-}$ cluster cell cycle analysis. Saos-2 cells in logarithmic growth phase were selected and separated into $CD133^+$ and $CD133^-$ subpopulation cells by the method described, fixed with 70% ice-cold ethanol for 24 h and treated with Triton X-100 (Sigma-Aldrich, St. Louis, MO, USA). Following PBS washing and centrifugation, 1 mg/ml RNase A (AppliChem Inc., St. Louis, MO, USA) was added to the cells and incubated for 15 min. Then, 50 μg/ml PI (Shanghai Jingmei Biotech, Shanghai, China) was added and cells were stained for 15 min. Cells were collected and analyzed using the FACSCalibur flow cytometer and Modfit software (Bio-Rad, Hercules, CA, USA) was used to analyze cell cycle stage.

Real-time polymerase chain reaction (PCR). TRIzol (1 ml) was added to the collected cell suspension (5-10x10^6 cells). Following homogenization, samples were incubated for 5 min at 15-30˚C to completely separate nucleic acid-protein complexes. $CHCl_3$ (0.2 ml; Shanghai Chemical Reagent, Shanghai, China) was added and the tubes were agitated by hand for 15 sec. Tubes were incubated for 2-3 min at 15-30˚C and then centrifuged at 12,000 x g for 15 min at 4˚C. Following centrifugation, the mixed solution was separated into 3 phases in which RNA was in the clear water phase. The water phase was transferred into a new centrifuge tube and mixed with 0.5 ml isopropanol (Shanghai Chemical Reagent) to completely precipitate RNA. The amount of added isopropanol was determined as follows: if 1 ml TRIzol was added

Table I. Primer sequences for real-time PCR.

Gene	Primer sequence	Product length (bp)
GAPDH	F: 5'AAGAAGGTGGTGAAGCAGGC3' R: 5'TCCACCACCCTGTTGCTGTA3'	203
MDR1	F: 5'CGGTTTGGAGCCTACTTGGT3' R: 5'GGTCGGGTGGGATAGTTGAATA3'	272
Sox2	F: 5'ATCACCCACAGCAAATGACA3' R: 5'CAAAGCTCCTACCGTACCACTA3'	245

MDR1, multidrug resistance protein 1; Sox2, sex determining region Y-box 2; PCR, polymerase chain reaction; F, forward; R, reverse.

to each sample to develop the homogenate, then the amount of isopropanol was 0.5 ml. The samples were incubated for 10 min at 15-30˚C and then centrifuged at 12,000 x g for 10 min at 4˚C. Before centrifugation, the invisible RNA precipitate formed gelatinous precipitate at the bottom and side wall of tube. The supernatant was removed and the precipitate was washed in 1 ml 75% ethanol (prepared with DEPC-treated water), agitated and centrifuged at 7,500 x g for 5 min at 4˚C. Ethanol was removed and the RNA precipitate was dried for 5-10 min in air. The RNA precipitate was not dried completely, to avoid reducing the solubility. The $A_{260/280}$ ratio of partly dissolved RNA samples was <1.6. RNA was dissolved in RNase-free water, incubated for 10 min at 55-60˚C and preserved at -70˚C. For extraction of low concentrations of RNA, 5-10 μg RNase-free glycogen (<4 mg/ml; Invitrogen Life Technolgies, USA) was added as water phase vector prior to the addition of isopropanol. To decrease the solution viscosity, the samples were passed through a 26-gauge syringe needle twice to slice genomic DNA prior to the addition of $CHCl_3$. After separating the two phases, glycogen remained in the water phase and coprecipitated with RNA.

Real-time (RT) reaction solution (10 μl) was added to 10 μl annealing mixture, incubated for 60 min in a 37˚C water bath, heated to 95˚C for 5 min and then placed in an ice bath. cDNA templates confirmed to express target and house-keeping genes were selected. PCR conditions were as follows: 95˚C for 3 min, 40 PCR cycles (94˚C for 20 sec, 59˚C for 20 sec and 72˚C for 30 sec) and 72˚C for 5 min. Products were run on a 2% agarose gel with a 100-bp DNA ladder and visualized with ethidium bromide to determine whether the correct gene was amplified. The PCR product (set as 1) was diluted to a series of concentrations. DNA templates of these gradient concentrations and all cDNA samples were respectively applied to prepare the real-time PCR system. Primer sequences and reaction conditions are presented in Table I.

The real-time PCR conditions were as follows: GAPDH, 95˚C for 5 min, 45 PCR cycles (95˚C for 10 sec, 59˚C for 15 sec, 72˚C for 20 sec and 83.8˚C for 5 sec); multidrug resistance protein 1 (MDR1), 95˚C for 5 min, 40 PCR cycles (95˚C for 10 sec, 59˚C for 15 sec, 72˚C for 20 sec and 81˚C for 5 sec); Oct4, 95˚C for 5 min, 45 PCR cycles (95˚C for 10 sec, 59˚C for 15 sec, 72˚C for 20 sec and 84˚C for 5 sec); Sox2, 95˚C for 5 min, 40 PCR cycles (95˚C for 10 sec, 59˚C for 15 sec, 72˚C for 20 sec, 81˚C for 5 sec); and Nanog, 95˚C for 5 min, 40 PCR cycles (95˚C for 10 sec, 59˚C for 15 sec, 72˚C for 20 sec, 81˚C for 5 sec). In order to establish the melting curve of the PCR products, the products were heated slowly from 72 to 99˚C (temperature increased by 1˚C every 5 sec) after the amplification reaction. Target and house-keeping genes of each sample were analyzed by real-time PCR to calculate gene concentrations by standard curve. The corrected relative content of the gene in the sample was calculated by dividing the house-keeping gene concentration by the target gene concentration in the sample.

Table II. Percentage of $CD133^+$ in the total cell population in various human osteosarcoma tissue specimens (mean ± SD).

Group	n	% $CD133^+$
1	4	5.63±1.96
2	13	6.54±1.65
3	12	8.54±1.25
4	26	13.84±3.81

CD133, cluster of differentiation.

$CD133^+$ cell colony-forming efficiency detection. Separated $CD133^{+/-}$ subpopulation cells were suspended in DMEM containing 20% FBS. The cell suspension was diluted and the cells were inoculated into culture dishes (diameter, 60 mm) containing 10 ml prewarmed medium (37˚C) at densities of 50, 100 and 200 cells/dish and cultured for 3 weeks at 37˚C, 5% CO_2 in a saturated humidity incubator. Following incubation, the cells were observed and counted to calculate the colony-forming efficiency using the following formula: Colony-forming efficiency (%) = no. of clones/no. of inoculated cells.

Cell cycle analysis following proliferation and differentiation of $CD133^+$ cells. $CD133^+$ subpopulation cells were inoculated into two culture flasks in DMEM containing 20% FBS and cultured at 37˚C, 5% CO_2 in a saturated humidity incubator. On day 3 and 7, the proportion of $CD133^+$ cells in the CD133 cell population was determined by flow cytometry. On day 7, the cells were collected to determine the cell cycle phase, with Saos-2 cells used as a control. All experiments were repeated three times.

Table III. Q-test comparison between osteosarcoma groups.

Group	Q-value	P-value
1 vs. 2	0.7858	>0.05
1 vs. 3	2.4756	>0.05
2 vs. 3	2.4481	>0.05
1 vs. 4	7.5055	<0.01[a]
2 vs. 4	10.5446	<0.01[a]
3 vs. 4	7.4552	<0.01[a]

[a]Statistically significant. Group 1, parosteal; Group 2, fibroblastic; Group 3, chondroblastic; Group 4, osteoblastic.

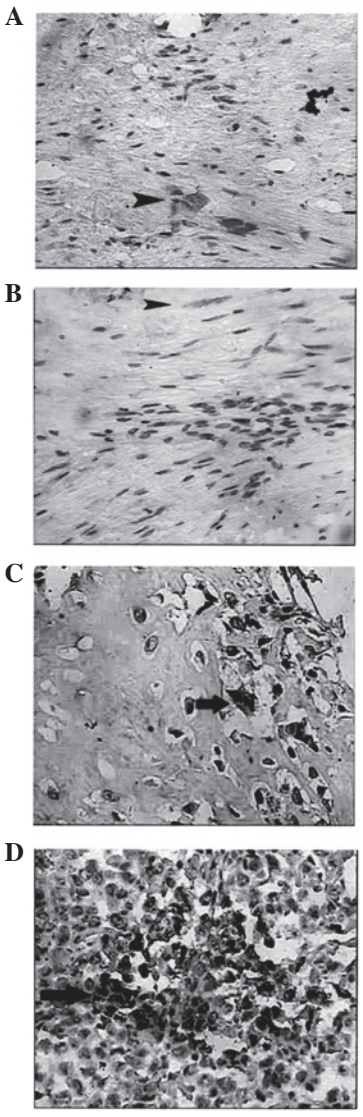

Figure 1. Immunohistochemical analysis of CD133 expression in human osteosarcoma tissues. (A) Parosteal; (B) fibroblastic; (C) chondroblastic; and (D) osteoblastic. CD133, cluster of differentiation.

Statistical analysis. All tests were repeated three times. Statistical analysis was carried out using the Student's t-test with SPSS software. P<0.05 was considered statistically significant.

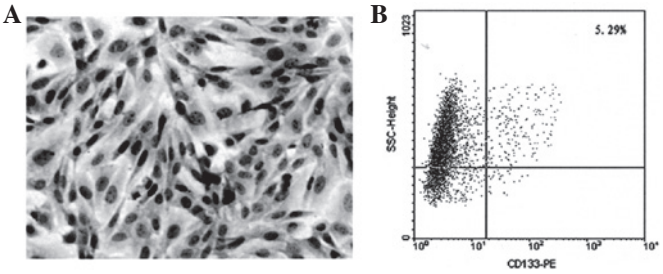

Figure 2. CD133 expression in the human Saos-2 cell line. (A) Immunohistochemical and (B) flow cytometry analysis. Analysis of flow cytometry data by Student's T-test revealed a result of 5.73±0.93 from 3 independent experiments. CD133, cluster of differentiation.

Results

CD133 expression in osteosarcoma. In the present study, $CD133^+$ cells were identified in various types of osteosarcoma (Fig. 1). Cell count analysis indicated that the $CD133^+$ ratio in parosteal, fibroblastic, chondroblastic and osteoblastic osteosarcoma was 5.63±1.96, 6.54±1.65, 8.54±1.25 and 13.84±3.81, respectively. Q-analysis identified no significant difference between $CD133^+$ ratios in parosteal, fibroblastic and chondroblastic osteocarcinomas (P>0.05). However, the ratio obtained in osteoblastic osteosarcomas was found to be significantly different compared with the other osteosarcoma groups (P<0.01; Tables II and III).

CD133 expression in Saos-2 cell lines. The results of the immunostaining performed in the Saos-2 cell line are presented in Fig. 2A. Analysis by flow cytometry revealed that a mean of 5.73±0.93% of cells were $CD133^+$ (Fig. 2B).

Cell cycle analysis of $CD133^+$ cells. Compared with Saos-2 cells, $CD133^+$ subgroup cells were identified in the G_0/G_1 stages of the cell cycle and exhibited a lower G_2 peak (Fig. 3). The percentage of Saos-2 cells in G_0/G_1, G_2/M and S stages was 48.86±1.09, 16.99±1.34 and 34.15±2.31, respectively, while $CD133^+$ subgroup cells were identified as significantly different at 79.09±1.61, 3.66±0.32 and 17.25±1.29, respectively (P<0.01; Table IV). The number of $CD133^+$ subpopulation cells was increased in G_0/G_1 and decreased in G_2/M and S stages compared with Saos-2 cells, indicating that $CD133^+$ subgroup cells were quiescent, while Saos-2 cells were proliferating.

After 10 days of culture in complete medium, $CD133^+$ subpopulation cell proliferation and cell cycle analyses indicated that cell percentages at G_0/G_1, G_2/M and S stages were 50.24±1.35, 16.09±3.78 and 33.67±4.81, respectively, and were observed to be significantly different compared with the percentages on day 0 (P<0.05). No significant difference in the mean cell percentages at G0/G1, G2/M and S stages compared with Saos-2 cells was noted (P>0.05; Table V). Following complete $CD133^+$ subgroup cell culture, the percentages of cells in the G_2/M and S stage increased significantly and the cell cycle shifted from proliferative to the quiescent G_0/G1 stage (P<0.05). These results indicate the differentiation abilities of $CD133^+$.

Cell proportion alterations following $CD133^+$ subgroup proliferation. Following isolation using magnetic beads,

Table IV. Cell cycle analysis of Saos-2 and CD133+ Saos-2 cells (mean ± SD).

Group	G_0/G_1 (%)	G_2/M (%)	S (%)
Saos-2	48.86±1.09	16.99±1.34	34.15±2.31
CD133+	79.09±1.61	3.66±0.32	17.25±1.29
P-value	0.001132157[a]	0.001801684[a]	0.005575029[a]

[a]P<0.05. CD133, cluster of differentiation.

Table V. Cell cycle comparative study prior to and following CD133+ Saos-2 cell culture in complete medium (mean ± SD).

Group	G_0/G_1 (%)	G_2/M (%)	S (%)
Day 0	79.09±1.61[a]	3.66±0.32[a]	17.25±1.29[a]
Day 10	50.24±1.35[a,b]	16.09±3.78[a,b]	33.67±4.81[a,b]
Saos-2 cells	48.86±1.09[b]	16.99±1.34[b]	34.15±2.31[b]

[a]P<0.05 and [b]P>0.05; Day 0 and 10 compared with Saos-2 cells, respectively. CD133, cluster of differentiation.

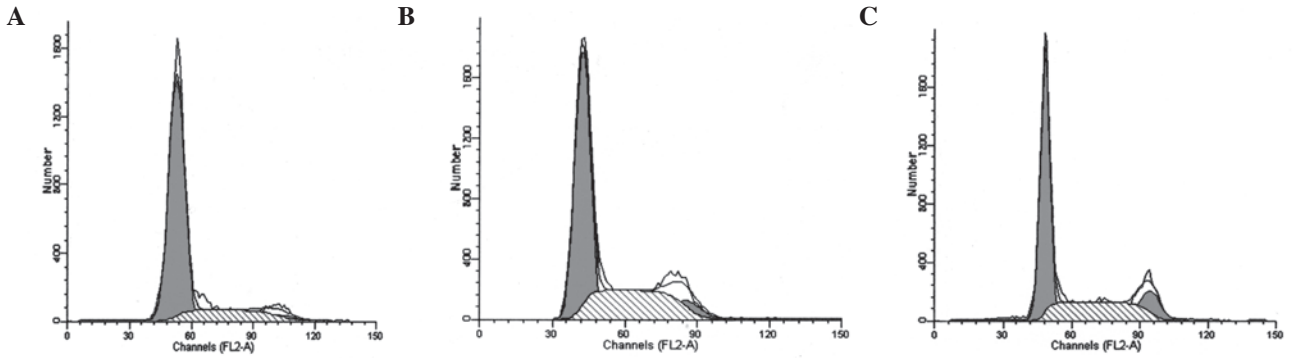

Figure 3. Cell cycle analysis. (A) CD133+ Saos-2 cells; (B) Saos-2 cells; and (C) CD133+ Saos-2 cells following culture in complete medium for 10 days. CD133, cluster of differentiation.

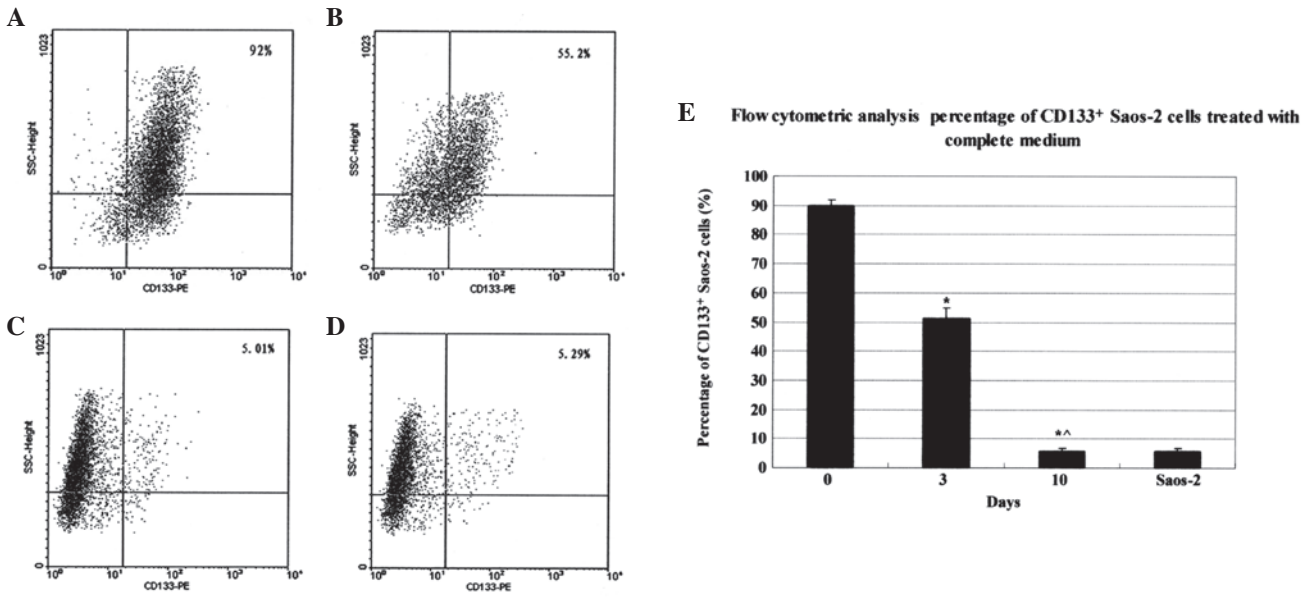

Figure 4. Flow cytometry analysis of CD133 prior to and following CD133+ Saos-2 cells culture in complete medium. Day (A) 0; (B) 3; (C) and 10; (D) Saos-2 cells; and (E) flow cytometry analysis of CD133 at days 0, 3 and 10 and in Saos-2 cells. Data are presented as mean ± SD of 3 independent experiments. *P<0.05, vs. day 0. ^P>0.05, vs. Saos-2. CD133, cluster of differentiation.

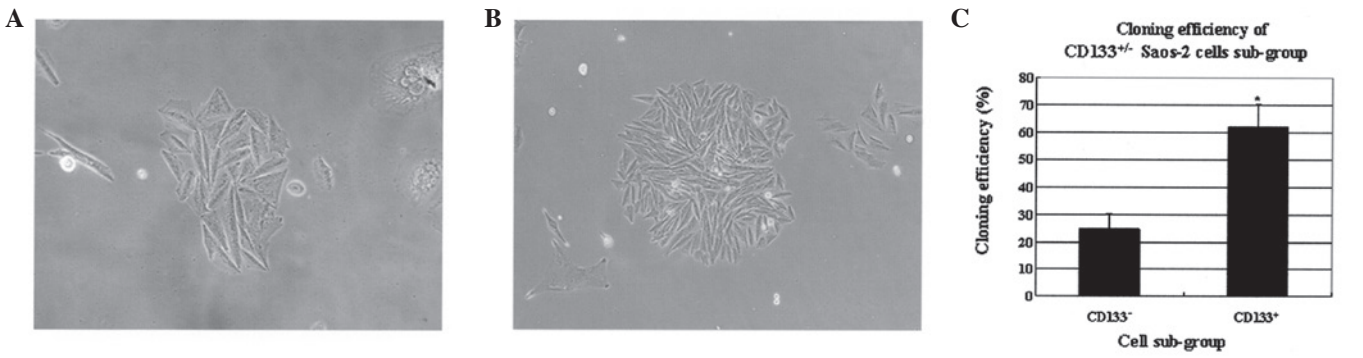

Figure 5. CD133$^{+/-}$ Saos-2 cell colony forming efficiency. (A) CD133^{-} Saos-2 cells (magnification, x40); (B) CD133^{+} Saos-2 cells (magnification, x20); and (C) cloning efficiencies of CD133$^{+/-}$ Saos-2 cells. Data are presented as the mean ± SD of 3 independent experiments. *P<0.05, vs. CD133^{-} Saos-2 cells. CD133, cluster of differentiation.

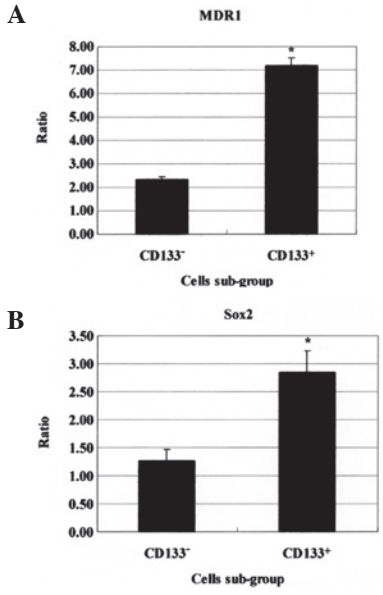

Figure 6. Real-time PCR analysis of MDR1 and Sox2 gene expression in CD133$^{-/+}$ Saos-2 cells. (A) MDR1; (B) Sox2. Data are presented as mean ± SD of 3 independent experiments. *P<0.05, vs. CD133^{-} cells. MDR1, multidrug resistance protein 1; Sox2, sex determining region Y-box 2; CD133, cluster of differentiation.

the percentage of CD133^{+} subgroup cells at day 0, 3 and 10 following cell culture was detected using flow cytometry as 90.02±1.75, 51.31±3.47 and 5.57±1.01, respectively. Statistical analysis indicated that the CD133^{+} cell percentage decreased significantly at days 3 and 10 compared with day 0 (90 to 5%), similar to that observed in the Saos-2 cells (Fig. 4). Results indicate the potential differentiation ability of VD133^{+} cells in complete culture medium.

Colony forming efficiency in CD133$^{+/-}$ subgroups. CD133^{+} cell colonies were larger compared with CD133^{-} cells following 5-week culture. The mean efficiencies of CD133^{+} and CD133^{-} subgroups, calculated from three repetitions, were 61.84±8.39 and 24.77±5.53, respectively, and were significantly different (P<0.05; Fig. 5).

Real-time PCR analysis of MDR1 and Sox2 gene expression. In CD133^{+} Saos-2 cells, Sox2 and MDR1 gene expression was identified to be significantly increased compared with CD133^{-} cells (P<0.05; Fig. 6).

Discussion

Cancer stem cells are defined as cancer cells with the ability to self-renew and divide into new tumorigenic cancer cells. Therefore, a single cancer stem cell has the ability to facilitate tumor metastasis and generate new tumors following transplantation. Current cancer stem cell hypotheses (1) classify tumors as a type of stem cell disease, an abnormal tissue generated by the proliferation of cancer stem cells with tumorigenic ability. The majority of tumor cells in tumor tissues have no or limited proliferative abilities, dying shortly following differentiation. However, a minority of cancer stem cells proliferate indefinitely, self-renew and have multiple differentiation potentials. Cancer stem cells may be critical for the formation, growth, infiltration, metastasis and recurrence of tumors (1,3). At present, a number of studies have demonstrated successful separation and identification of cancer stem cells in cancer tissues, including breast, lung, pancreatic, liver, prostate and colon cancers, malignant melanoma, retinoblastoma, brain tumors and head and neck squamous cell carcinoma, using specific markers whose functions were correlated with immunity on the surface of cells and associated techniques (21,25-28).

Self-renewal and differentiation potential are two key properties of cancer stem cells. Division during these processes has been identified as dissymmetric, whereby one daughter cells has the same undifferentiated state as the mother cell and cell cycle is at G_0 stage and the other develops oriented differentiation, with a cell cycle at G_2 and S stages. The daughter cells exhibit differentiation characteristics and associated markers. The majority of cancer stem cells are found at the G_0 stage (4,29,30).

The tumorigenicity of cancer stem cells varies significantly between various types of tumor, which is principally evaluated by two observations: i) the clonogenic ability of cancer stem cells *in vitro* i.e., the number and size of cancer stem cells clones derived from primary cancer tissues or tumor cell lines formed in soft agar or matrigel; and ii) the tumorigenic ability of cancer stem cells in immunodeficient animals by inoculating the same number of separated cancer

and non-cancer stem cells into immunodeficient animals and analyzing tumor formation, i.e., by counting the number of animals forming tumors and comparing the size of the formed tumors. The strongest tumorigenicity reported to date is brain cancer stem cells, whereby NOD/SCID mice inoculated with 100 $CD133^+$ cancer stem cells developed tumors 6 months following inoculation. No tumors formed in mice inoculated with $1x10^5$ $CD133^-$ non-cancer stem cells (5).

Drug resistance is one of the key properties of cancer stem cells and a number of studies have hypothesized that cancer stem cells are the principal cause of failure of tumor chemotherapy. Under normal conditions, the majority of drug-resistant molecules, including P-glycoprotein, multidrug resistance protein (MRP) 1, MRP2 and ATP-binding cassette transporter G2 (ABCG2), are expressed at various levels in epithelial cells of tissues of nutritional absorption (i.e., lung and digestive tract) and metabolic and emunctory organs (i.e., liver and kidney). These transport molecules are important for sustaining physiological barriers (blood-brain, blood-cerebrospinal fluid, blood-testis and mother-infant barriers and the placenta). ABC transporters are associated with regulation of absorption, nutrition distribution, metabolism, secretion and exogenous toxic substances (31,32). A previous study (30) in ABCG2 gene knockout mice noted bone marrow and skeletal muscle SP cells were significantly decreased and extremely low levels of Lin^-/c-Kit^+/$Sca\text{-}1^+$ SP cells were observed in bone marrow. Transplantation results of remaining SP cells revealed exhausted regeneration abilities and enhanced sensitivity of $Bcrp1^{-/-}$ hematopoietic cells to the anticancer drug mitoxantrone, indicating that ABCG2 expression is essential for SP phenotype of normal bone marrow stem cells. The majority of ABC transporter family membrane proteins are expressed on the membrane of almost all cancer stem cells and transport and excrete multiple substances, including metabolites, drugs, toxic substances, endogenous lipids, polypeptides, nucleotides and sterols (33), leading to a considerable decrease in the efficacy of a number of chemotherapies. Currently, studies on ABCG2 are important for understanding drug resistance in cancer stem cells and may lead to the development of new therapeutic strategies (9).

As CD133 is the most extensive marker in tumor progenitor cells, expression of CD133 in osteosarcoma cell lines was determined in the present study. $CD133^+$ Saos-2 cells were isolated using magnetic beads and the cell cycle, differentiation potential, cloning efficiency and MDR1 and Sox2 gene expression were analyzed. Percentage of $CD133^+$ in the total cell population in parosteal, fibroblast and chondroblast osteosarcomas was 5-8%, while in osteoblast osteosarcoma the $CD133^+$ subpopulation was ~13%, indicating that all types of osteosarcoma comprise small numbers of $CD133^+$ cells. Q-analysis indicated that the percentage of $CD133^+$ in the osteoblast type was higher than the other types. In the current study, percentage of $CD133^+$ cells in the total cell population in human osteosarcoma Saos-2 cells was 5%, 80% of which were at G_0/G_1 phase, while only 48% of total Saos-2 cells were in this phase and 50% were in G_2/M and S phases, indicating that Saos-2 cells were proliferating, however, $CD133^+$ Saos-2 cells were quiescent.

$CD133^+$ cells were separated and analyzed by flow cytometry. $CD133^+$ cells accounted for 90.02±1.75% in the separated population and this percentage rapidly declined to 51.31±3.47% and 5.57±1.01% following culture in complete medium for 3 and 10 days, respectively. Cell cycle analysis on day 10 found significant differences in cell distribution within phases compared with day 0 following separation and was similar to Saos-2 cells. These observations indicate that following culture in complete medium, $CD133^+$ cells differentiated and began proliferating, entering G_2/M and S stages. Analysis of cell colony formation observed that the colonies formed by the $CD133^+$ subpopulation were larger compared with $CD133^-$ and colony-forming efficiency, an important marker of tumorigenicity, was markedly increased, indicating that tumorigenicity of $CD133^+$ cells was higher than that of $CD133^-$ cells.

In the present study, $CD133^+$ Saos-2 cells were observed to make up a small percentage of the total Saos-2 cell population. In addition, $CD133^+$ cells exhibited a number of cancer stem cell characteristics, including quiescence and a marked differentiation potential, as well as expression of key stem cell regulatory and drug resistance genes, which may cause osteocarcinoma and high drug resistance.

Acknowledgements

The present study was supported by a grant from the National Natural Science Foundation of China (no. 30973018).

References

1. Reya T, Morrison SJ, Clarke MF and Weissman IL: Stem cells, cancer and cancer stem cells. Nature 414: 105-111, 2001.
2. Huntly BJ and Gilliland DG: Leukaemia stem cells and the evolution of cancer-stem-cell research. Nat Rev Cancer 5: 311-321, 2005.
3. Marx J: Cancer research. Mutant stem cells may seed cancer. Science 301: 1308-1310, 2003.
4. Al-Hajj M, Wicha M S, Benito-Hernandez A, *et al*: Prospective identification of tumorigenic breast cancer cells. Proc Natl Acad Sci USA 100: 3983-3988, 2003.
5. Singh SK, Hawkins C, Clarke ID, *et al*: Identification of human brain tumour initiating cells. Nature 432: 396-401, 2004.
6. Goodell MA, Brose K, Paradis G, *et al*: Isolation and functional properties of murine hematopoietic stem cells that are replicating in vivo. J Exp Med 183: 1797-1806, 1996.
7. Meyers PA, Schwartz CL, Krailo M, *et al*: Osteosarcoma: a randomized, prospective trial of the addition of ifosfamide and/or muramyl tripeptide to cisplatin, doxorubicin and high-dose methotrexate. J Clin Oncol 23: 2004-2011, 2005.
8. Budak-Alpdogan T, Banerjee D and Bertino JR: Hematopoietic stem cell gene therapy with drug resistance genes: an update. Cancer Gene Ther 12: 849-863, 2005.
9. Dean M, Fojo T and Bates S: Tumour stem cells and drug resistance. Nat Rev Cancer 5: 275-284, 2005.
10. Donnenberg VS and Donnenberg AD: Multiple drug resistance in cancer revisited: the cancer stem cell hypothesis. J Clin Pharmacol 45: 872-877, 2005.
11. Gerson SL: Drug resistance gene transfer: Stem cell protection and therapeutic efficacy. Exp Hematol 28: 1315-1324, 2000.
12. Richardson C and Bank A: Preselection of transduced murine hematopoietic stem cell populations leads to increased long-term stability and expression of the human multiple drug resistance gene. Blood 86: 2579-2589, 1995.
13. Gibbs CP, Kukekov VG, Reith JD, *et al*: Stem-like cells in bone sarcomas: implications for tumorigenesis. Neoplasia 7: 967-976, 2005.
14. Yin AH, Miraglia S, Zanjani ED, *et al*: AC133, a novel marker for human hematopoietic stem and progenitor cells. Blood 90: 5002-5012, 1997.
15. Lee A, Kessler JD, Read TA, *et al*: Isolation of neural stem cells from the postnatal cerebellum. Nat Neurosci 8: 723-729, 2005.

16. Sagrinati C, Netti GS, Mazzinghi B, *et al*: Isolation and characterization of multipotent progenitor cells from the Bowman's capsule of adult human kidneys. J Am Soc Nephrol 17: 2443-2456, 2006.
17. Richardson GD, Robson CN, Lang SH, *et al*: CD133, a novel marker for human prostatic epithelial stem cells. J Cell Sci 117: 3539-3545, 2004.
18. Kordes C, Sawitza I, Müller-Marbach A, *et al*: CD133^{+} hepatic stellate cells are progenitor cells. Biochem Biophys Res Commun 352: 410-417, 2007.
19. Sugiyama T, Rodriguez RT, McLean GW and Kim SK: Conserved markers of fetal pancreatic epithelium permit prospective isolation of islet progenitor cells by FACS. Proc Natl Acad Sci USA 104: 175-180, 2007.
20. Ito Y, Hamazaki TS, Ohnuma K, *et al*: Isolation of murine hair-inducing cells using the cell surface marker prominin-1/CD133. J Invest Dermatol 127: 1052-1060, 2007.
21. Collins AT, Berry PA, Hyde C, *et al*: Prospective identification of tumorigenic prostate cancer stem cells. Cancer Res 65: 10946-10951, 2005.
22. Yin S, Li J, Hu C, *et al*: CD133 positive hepatocellular carcinoma cells possess high capacity for tumorigenicity. Int J Cancer 120: 1444-1450, 2007.
23. Hermann PC, Huber SL, Herrler T, *et al*: Distinct populations of cancer stem cells determine tumor growth and metastatic activity in human pancreatic cancer. Cell Stem Cell 1: 313-323, 2007.
24. Eramo A, Lotti F, Sette G, *et al*: Identification and expansion of the tumorigenic lung cancer stem cell population. Cell Death Differ 15: 504-514, 2008.
25. Kim CF, Jackson EL, Woolfenden AE, *et al*: Identification of bronchioalveolar stem cells in normal lung and lung cancer. Cell 121: 823-835, 2005.
26. Fang D, Nguyen TK, Leishear K, *et al*: A tumorigenic subpopulation with stem cell properties in melanomas. Cancer Res 65: 9328-9337, 2005.
27. Ricci-Vitiani L, Lombardi DG, Pilozzi E, *et al*: Identification and expansion of human colon cancer initiating cells. Nature 445: 111-115, 2007.
28. Prince ME, Sivanandan R, Kaczorowski A, *et al*: Identification of a subpopulation of cells with cancer stem cell properties in head and neck squamous cell carcinoma. Proc Natl Acad Sci USA 104: 973-978, 2007.
29. Chambers I and Smith A: Self-renewal of teratocarcinoma and embryonic stem cells. Oncogene 23: 7150-7160, 2004.
30. Pan CX, Zhu W and Cheng L: Implications of cancer stem cells in the treatment of cancer. Future Oncol 2: 723-731, 2006.
31. Leslie EM, Deeley RG and Cole SP: Multidrug resistance proteins: role of P-glycoprotein, MRP1, MRP2 and BCRP (ABCG2) in tissue defense. Toxicol Appl Pharmacol 204: 216-237, 2005.
32. Dietrich CG, Geier A and Oude Elferink RP: ABC of oral bioavailability: transporters as gatekeepers in the gut. Gut 52: 1788-1795, 2003.
33. Staud F and Pavek P: Breast cancer resistance protein (BCRP/ABCG2). Int J Biochem Cell Biol 37: 720-725, 2005.